

# Development of New $\text{Cd}^{2+}$ and $\text{Pb}^{2+}$ Lennard-Jones Parameters for Liquid Simulations

Alexandre S. de Araujo,<sup>\*,†</sup> Milton T. Sonoda,<sup>†</sup> Oscar E. Piro,<sup>‡</sup> and Eduardo E. Castellano<sup>†</sup>

*Instituto de Física de São Carlos, Universidade de São Paulo, Cx.P. 369 São Carlos, SP, 13566-590, Brazil, and Departamento de Física, Facultad de Ciencias Exactas, Universidad Nacional de La Plata and IFLP (CONICET), C.C. 67, 1900, La Plata, Argentina*

*Received: July 28, 2006; In Final Form: November 27, 2006*

We present new Lennard-Jones parameters for  $\text{Cd}^{2+}$  and  $\text{Pb}^{2+}$  ion–water interactions and describe a general methodology to obtain these parameters for any ion. Our strategy is based on the adjustment of ion parameters to reproduce simultaneously experimental absolute hydration free energy and structural properties, namely,  $g(r)$  and coordination numbers, obtained from X-ray liquid scattering and quantum mechanical/molecular mechanical (QM/MM) calculations. The validation of the obtained parameters is made by the calculation of dynamical properties and comparing them with experimental values and theoretical results from the literature. The transferability of parameters is checked by the calculation of thermodynamic, structural, and dynamical properties cited above with four different water models. The results obtained for  $\text{Cd}^{2+}$  and  $\text{Pb}^{2+}$  show an overall agreement with reference values. The absolute hydration free energy calculated with the TIP3P, SPC/E, SPC, and TIP4P water models presents, respectively, percent differences of 3.8, 3.0, 4.3, and 7.2% for lead(II) and 9.8, 8.4, 10.2, and 14.1% for cadmium(II) when compared with experimental values. Ion–water mean distance and coordination numbers for the first coordination shell are in good agreement with experimental and QM/MM results for both ions.  $\text{Cd}^{2+}$  shows a lesser diffusion coefficient compared to that of  $\text{Pb}^{2+}$  despite its smaller atomic radius, indicating a more persistent first coordination shell for the cadmium(II) ion, a result confirmed with calculations of the mean residence time of water molecules in the first coordination shell.

## Introduction

Contamination by heavy metals is of worldwide concern, particularly in the cases of cadmium and lead.<sup>1–4</sup> The inappropriate discard of batteries, extensive use of herbicides and fungicides, gasoline burn, and several industrial processes are the main cause of pollution. The presence of those metals in living organisms may cause severe intoxication, a process that could be enhanced by biomagnification, leading to contamination all along the food chain.<sup>5,6</sup> In humans, the main source of intoxication by Cd and Pb occurs through the ingestion of food and also smoking.<sup>7–10</sup>

Despite the efforts to reduce heavy metals emission, the level of contamination in several environments remains too high. This risky scenario for the biomass prompts the resort to chemical processes to remove these metals or, at least, render them into an inert chemical.<sup>11</sup> In this context, it is of interest to study the physical chemistry behavior of  $\text{Cd}^{2+}$  and  $\text{Pb}^{2+}$  ions in solution with the aim to develop efficient extraction processes of these contaminants from water.

Molecular dynamics (MD) simulations provide useful information from a molecular perspective of the dynamical processes taking place in aqueous solutions of heavy ions. The possibility to follow the behavior and organization of solute and solvent at the atomic resolution renders this technique a useful tool to assist detailed physical chemistry studies. To this purpose, it is necessary to accurately model the intermolecular interactions in an attempt to closely mimic the behavior of real solutions.

Particularly, MD simulations of contaminant  $\text{Cd}^{2+}$  and  $\text{Pb}^{2+}$  ions in water solutions could provide useful information on the behavior of these metals in natural environments.

Parameters describing the metal–solvent interaction for alkaline and alkaline-earth ions, halides, and some transition and lanthanide metals are reported in the literature.<sup>12–15</sup> In general, these parameters are determined to reproduce the observed thermodynamic, structural, and dynamical properties of these elements in water solutions. Until recently, the only available interaction models for  $\text{Cd}^{2+}$  and  $\text{Pb}^{2+}$  ions were developed for the MM3<sup>16</sup> and UFF<sup>17</sup> force fields which, however, are not appropriate for liquid simulations. Prompted by these difficulties, Lim and Babu<sup>18</sup> developed a procedure by which the Lennard-Jones parameters of several divalent cations are obtained from interpolation of calculated relative hydration free energy curves.

Following the methodology proposed by Aqvist,<sup>12</sup> we developed and report here new Lennard-Jones parameters for  $\text{Cd}^{2+}$  and  $\text{Pb}^{2+}$  ion–water van der Waals interactions, adjusting them to simultaneously reproduce thermodynamic and structural properties from available experimental and quantum mechanical/molecular mechanical (QM/MM) data. The Lennard-Jones function for dispersive interaction is widely used in molecular liquid simulations and is currently implemented in several force fields (e.g., OPLS,<sup>19</sup> GROMOS,<sup>20</sup> and AMBER<sup>21</sup>). The new parameters were developed with the TIP3P<sup>22</sup> water model. In order to test the transferability of the obtained parameters, we also computed the absolute solvation free energies and structural properties employing the SPC,<sup>23</sup> SPC/E,<sup>24</sup> and TIP4P<sup>22</sup> water models. The dynamical behavior of our models was assayed by computing the self-diffusion coefficients of the ions, and

\* To whom correspondence should be addressed. E-mail: asaraujo@ifsc.usp.br. Fax: 55+16+3373-9881.

<sup>†</sup> Universidade de São Paulo.

<sup>‡</sup> Universidad Nacional de La Plata and IFLP (CONICET).

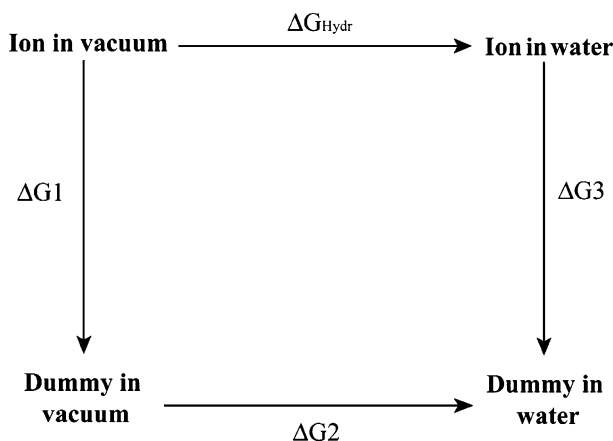


**Figure 1.** Thermodynamic cycle for hydration free energy calculations.

the results were compared with experimental data. Mean residence times were also computed to have a better understanding of the solvation process of the solute.

### Methodology

The parametrization of the Lennard-Jones function (eq 1) for the  $\text{Cd}^{2+}$  and  $\text{Pb}^{2+}$  ions follows the work by Aqvist<sup>12</sup> in his study on alkaline and alkaline-earth ions in solution. However, we employed the TIP3P water model and the linear interaction energy (LIE)<sup>25</sup> method rather than the free energy perturbation (FEP)<sup>26</sup> one for the hydration free energy calculations. Initial calculations of hydration free energy using original ion parameters from UFF adapted to OPLS did not reproduce the available experimental data. The parameters were then refined to reproduce simultaneously available experimental absolute hydration free energy,  $\Delta G_{\text{Hydr}}$ ,<sup>27</sup> and structural properties obtained from X-ray scattering<sup>28</sup> and QM/MM simulations.<sup>29,30</sup> Ion hydration structures were analyzed through the radial distribution function,  $g(r)$ . The  $g(r)$  function and  $\Delta G_{\text{Hydr}}$  free energies were also computed with the SPC, SPC/E, and TIP4P water models to investigate the transferability of the new parameters. Concerning dynamic behavior, we computed the self-diffusion coefficient for ions in solution through the well-known Einstein relation<sup>31</sup> and the persistence of the hydration shell from calculation of the mean residence time following the method proposed by Impey et al.<sup>32</sup>

$$U_{ij} = 4\epsilon_{ij} \left[ \left( \frac{\sigma_{ij}}{r_{ij}} \right)^{12} - \left( \frac{\sigma_{ij}}{r_{ij}} \right)^6 \right] \quad (1)$$

To calculate the hydration free energy, we used the thermodynamic cycle shown in Figure 1.

Since  $\Delta G1 = \Delta G2 = 0$ , it turns out that the thermodynamic cycle reduces to  $\Delta G_{\text{Hydr}} = -\Delta G3$ , and therefore, the initial state (A) consists of the dummy atom in water and the final state (B) refers to the ion in water.

The absolute hydration free energy of the ions was obtained through the following relation:

$$\Delta G_{\text{Hydr}}(I^{n+}) = \Delta G_{\text{SR}}(I^0 \rightarrow I^{n+}) + \Delta G_{\text{Born}} + \Delta G_{\text{Cav}} \quad (2)$$

The short-range interaction contribution to the hydration free energy of ions,  $\Delta G_{\text{SR}}$ , usually reaches thousands of kJ/mol. These energy scales make the use of thermodynamic methods, such as FEP<sup>26</sup> and thermodynamic integration (TI),<sup>33</sup> unfeasible due to the large number of simulations required to obtain a good overlap in phase space between consecutive intermediate

states.<sup>34</sup> In these cases, the LIE method is more convenient because it only needs sampling of the initial and final states and therefore it does not demand large computational resources to deal with intermediate configurations.<sup>25,35</sup> The semiempirical LIE method was originally developed to calculate the absolute free energies involved in macromolecule–ligand binding and hydration free energies and is based on the so-called linear response approximation for electrostatic forces.<sup>25</sup> In this method, the difference between the free energy of two states A and B is computed through the following expression:

$$\Delta G_{\text{bind}} = \frac{1}{2}(\langle V_{i-s}^{\text{el}} \rangle_{\text{B}} - \langle V_{i-s}^{\text{el}} \rangle_{\text{A}}) + \alpha(\langle V_{i-s}^{\text{vdw}} \rangle_{\text{B}} - \langle V_{i-s}^{\text{vdw}} \rangle_{\text{A}}) \quad (3)$$

where  $\langle V_{i-s}^{\text{el}} \rangle_Y$  and  $\langle V_{i-s}^{\text{vdw}} \rangle_Y$  are, respectively, the mean of electrostatic and van der Waals interaction between the ion (i) and solvent (s) in state Y. The  $1/2$  factor in the equation is obtained from the linear response approximation, and the  $\alpha$  parameter, which was obtained empirically from MD calculations in nonpolar solvents, takes the value 0.181 in this work.<sup>36</sup> The mean energy values in eq 3 are obtained from MD simulations carried on the A and B states. In the case of the solvated ion, the A state corresponds to a dummy atom in water, leading to  $V_{\text{A}} = 0$ , and consequently, our hydration free energy calculation involves a single simulation, namely, the ion in water. The LIE method was employed to compute the  $\Delta G_{\text{SR}}$  value of eq 2, with interaction terms contributing to average values only when the ion–water distance is below a given cutoff.

The contribution to the free energy due to the solvent molecules beyond the cutoff radius (surrounding infinite medium) was evaluated by means of the Born formula,<sup>12</sup> which (in kJ/mol) is given by

$$\Delta G_{\text{Born}} = \frac{-1347(1 - \epsilon^{-1})q^2}{2r_{\text{Born}}} \quad (4)$$

where  $\epsilon$  is the solvent dielectric constant,  $q$  is the solute charge (in number of electrons), and  $r_{\text{Born}}$  (in Å units) is the cutoff radius. The Born contribution affects only absolute free energies, and it cancels out when calculating relative free energies. The Born approach has shown to give fine results for sufficiently large cutoff radii (see Computational Details). Other long-range electrostatic interaction treatments, such as reaction field and Ewald summation, could be employed. However, we chose to use Born's formula to maintain the consistency between our parameters and the whole set of already developed<sup>12</sup> ones for the divalent cations widely used in the literature. The  $\Delta G_{\text{Cav}}$  term corresponds to the free energy necessary to create a cavity in the solvent to accommodate the ion and can be safely neglected, as it turns out to be of the order of a few kJ/mol and, therefore, well within the estimated errors.<sup>37</sup>

The structural hydration properties were analyzed through the radial distribution function,  $g_{ij}(r)$ ,

$$g_{ij}(r) = \frac{\langle N_j(r, r+\Delta r) \rangle}{\rho_j 4\pi r^2 \Delta r} \quad (5)$$

where  $N_j(r, r+\Delta r)$  is the mean number of  $j$ -atoms in the spherical shell within the  $r$  and  $r + \Delta r$  radii centered on the  $i$  atom and  $\rho_j$  is the  $j$ -atoms numeric density. The ion–water  $g(r)$  distribution function was calculated from simulation trajectories. This function, in turn, provided information on the average distances of solvation shells and coordination numbers.

The computation of dynamical properties was based on the work by Impey et al.<sup>32</sup> We determine the ion self-diffusion coefficients,  $D_{\text{ion}}$ , and the mean residence time of the solvent molecules in their first coordination shell,  $\tau_{\text{ion}}$ .  $D_{\text{ion}}$  was calculated from the mean square displacement (MSD) of the ion,  $\langle |\vec{R}(t) - \vec{R}(0)|^2 \rangle$ , through the Einstein relation

$$6D_{\text{ion}} = \lim_{t \rightarrow \infty} \frac{d}{dt} \langle |\vec{R}(t) - \vec{R}(0)|^2 \rangle \quad (6)$$

The  $g(r)$  function characterizes the time-averaged structure of the solvation shells and therefore provides a static picture of the coordination process. However, solvation has a dynamical nature, since individual solvent molecules are constantly entering and leaving the ion coordination environment. This temporal process can be quantified by a *survival probability function*,  $S(t)$ , defined as

$$S(t) = \frac{1}{N} \left\langle \sum_{j=1}^M P_j(t_0, t+t_0; t^*) \right\rangle_{t_0} \quad (7)$$

where  $M$  is the total number of solvent molecules,  $\langle \mathbf{O} \rangle_{t_0}$  represents the temporal average of  $\mathbf{O}$ ,  $N$  is the mean coordination number, and  $P_j(t_0, t+t_0; t^*)$  is the probability of a solvent molecule,  $j$ , being in the solvation shell at time  $t+t_0$  assuming that it was already in the solvation shell at time  $t_0$  and in this interim it did not leave the shell in a time greater than  $t^*$ . Except for short times, the  $S(t)$  function decay can be suitably fitted by the exponential function  $\exp(-t/\tau_{\text{ion}})$ , from which a characteristic residence time,  $\tau_{\text{ion}}$ , is obtained.<sup>32</sup>

### Computational Details

The MD simulations were carried out using the GROMACS<sup>38</sup> package with the OPLS-AA<sup>19</sup> force field. The reliability of the LIE method was tested by calculating the hydration free energy for the ions Ca<sup>2+</sup>, Sr<sup>2+</sup>, and Ba<sup>2+</sup> and comparing the results with corresponding experimental values reported in the literature.<sup>27</sup>

The Cd<sup>2+</sup> and Pb<sup>2+</sup> ions were modeled taking as initial parameters the ones obtained with the UFF<sup>17</sup> force field. The ions were placed in the center of a previously equilibrated cubic box with an edge length equal to 35 Å containing 1409 TIP3P water molecules. For each ion, we performed a 500 ps simulation for equilibration followed by another calculation lasting 5 ns for data acquisition, both with 1 fs time steps. Pressure and temperature were kept at constant values of 1 bar and 300 K (NPT ensemble), respectively, employing the Berendsen algorithms with time constants of 1.0 and 0.1 ps. We applied periodic boundary conditions and a cutoff radius of 15 Å for the Coulomb and van der Waals short-range interactions. The long-range Coulombic interaction was not computed, and its contribution to the free energy was estimated with Born's formula (eq 4) using  $\epsilon = 78$  and an  $r_{\text{Born}}$  value equal to the cutoff distance. We also applied cutoffs of 10 and 17 Å to verify its influence on hydration free energies, obtaining essentially the same results.

After carrying out the necessary MD simulations, employing the TIP3P model for the water molecules, we obtained the parameters for the Cd<sup>2+</sup> and Pb<sup>2+</sup> ions that better reproduce simultaneously experimental absolute hydration free energy data and structural properties from X-ray scattering or QM/MM calculations. To verify the transferability of the obtained parameters, we also computed these properties for other water models, namely, TIP4P, SPC, and SPC/E. We then derived the

TABLE 1: Final Lennard-Jones Parameters

ion	$\sigma$ (Å)	$\epsilon$ (kJ/mol)
Pb <sup>2+</sup>	3.0	0.800
Cd <sup>2+</sup>	2.7	0.025

TABLE 2: Calculated, Experimental, and Relative Error for Hydration Free Energies

ion	$\Delta G_{\text{calcd}} \pm 10$ (kJ/mol)	$\Delta G_{\text{exptl}}^a$ (kJ/mol)	water model	error (%)
Ca <sup>2+</sup>	-1534	-1593.27	TIP3P	3.7
Sr <sup>2+</sup>	-1439	-1447.25	TIP3P	0.5
Ba <sup>2+</sup>	-1339	-1318.38	TIP3P	1.5
Pb <sup>2+</sup>	-1440	-1497.04	TIP3P	3.8
Pb <sup>2+</sup>	-1433	-1497.04	SPC	4.3
Pb <sup>2+</sup>	-1451	-1497.04	SPC/E	3.0
Pb <sup>2+</sup>	-1389	-1497.04	TIP4P	7.2
Cd <sup>2+</sup>	-1624	-1801.21	TIP3P	9.8
Cd <sup>2+</sup>	-1618	-1801.21	SPC	10.2
Cd <sup>2+</sup>	-1650	-1801.21	SPC/E	8.4
Cd <sup>2+</sup>	-1548	-1801.21	TIP4P	14.1

<sup>a</sup> Reference 27.

solution dynamical properties for all four water models from 5 ns MD trajectories. The solvation shell boundaries, obtained from  $g(r)$ , were used in the calculation of  $S(t)$ .

### Results and Discussion

**Absolute Hydration Free Energies of Ions.** Hydration free energies of Ca<sup>2+</sup>, Sr<sup>2+</sup>, and Ba<sup>2+</sup> OPLS ions in the TIP3P water model computed from eq 2 are presented in Table 2 along with experimental data. The good agreement between them shows the reliability of the employed methodology. An observed systematic trend of the smaller radius divalent ions to have a more negative hydration free energy indicates a stronger interaction with the water molecules in the first coordination shell around the ion. The final Lennard-Jones parameters for Cd<sup>2+</sup> and Pb<sup>2+</sup> ions are shown in Table 1. The hydration free energies calculated for the four water models considered are included in Table 2.

To estimate the numerical errors, we divided the 5 ns trajectory into five equal parts and calculated the corresponding  $\Delta G_{\text{Hydr}}$  value from them. The standard deviations were below 3 kJ/mol. However, since we are neglecting the  $\Delta G_{\text{Cav}}$  contribution, which is about 10 kJ/mol for cavities with a radius around 3 Å,<sup>37</sup> we took the latter value as the estimated error of our calculations. For the Pb<sup>2+</sup> ion, the calculated hydration free energies are in overall good agreement with the experimental results<sup>27</sup> for all considered water models. The error is about 3.7% for the TIP3P, SPC, and SPC/E water models and 7.2% for the TIP4P model. Though the comparison between calculated and experimental data for Cd<sup>2+</sup> is not as good as that for Pb<sup>2+</sup>, the parametrization of the former ion can still be considered satisfactory. The corresponding percent differences as compared with experimental free energies are 9.8% for the TIP3P model, 8.4% for SPC/E, 10.2% for SPC, and 14.1% for TIP4P. We notice that for both ions the best agreement with experimental data is obtained with the TIP3P and SPC/E water models. The MD simulations with the water TIP4P model lead to the largest differences with experimental values, reaching the above-mentioned error of 14.1% in the hydration free energy of the Cd<sup>2+</sup> ion. This discrepancy may be due to the fact that in adjusting our Lennard-Jones parameters the TIP3P model uses three interacting sites rather than the four used in the TIP4P water model.

The hydration free energy of the Cd<sup>2+</sup> ion turns out to be about 250 kJ/mol more negative than the value obtained for

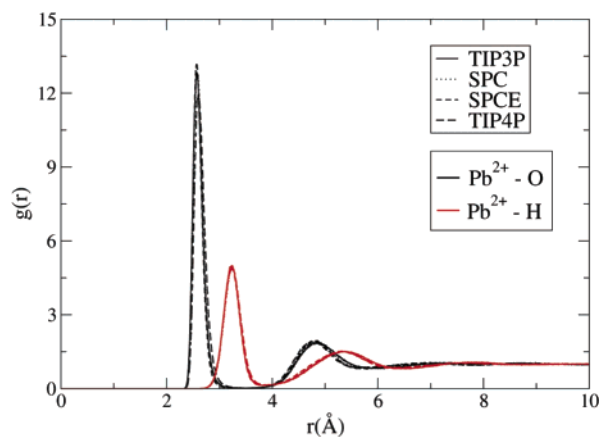


**Figure 2.** Radial distribution function,  $g(r)$ , of  $\text{Pb}^{2+}$ -O and  $\text{Pb}^{2+}$ -H for the four water models used.

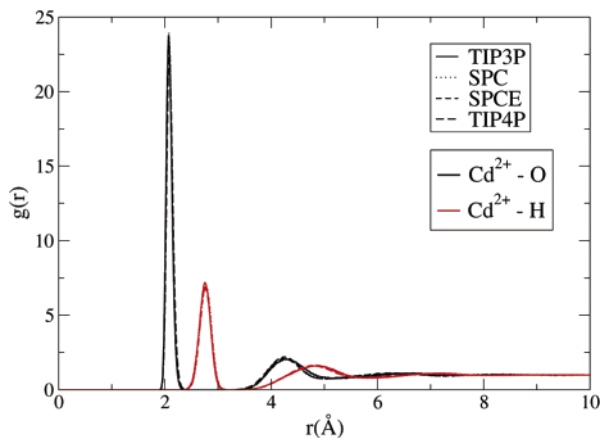


**Figure 3.** Radial distribution function,  $g(r)$ , of  $\text{Cd}^{2+}$ -O and  $\text{Cd}^{2+}$ -H for the four water models used.

the  $\text{Pb}^{2+}$  ion, showing a stronger solvation for the former ion as compared with the latter one. This striking difference is confirmed by the calculated structural and dynamical properties.

**Structural Properties.** The radial pair distribution function,  $g(r)$ , provides structural information on the solvation shells around the ion, namely, the mean ion-solvent distances and coordination numbers. We calculated the  $g(r)$  function between  $\text{Pb}^{2+}$  and  $\text{Cd}^{2+}$  ions and  $\text{O}_w$  and  $\text{H}_w$  atoms for all considered water models, and the results are shown in Figures 2 and 3. It can be seen that the distribution functions are practically identical for all four water models, and therefore, in what structural properties concern, our Lennard-Jones parameters can safely be considered transferable.

The  $g(r)$  function for the  $\text{Cd}^{2+}$  ion displays a sharp first peak and a well-defined minimum for both the ion- $\text{O}_w$  and ion- $\text{H}_w$  distances, thus suggesting a well-defined first hydration shell with much reduced molecular exchange with the solvent bulk. The  $g(r)$  distribution function for the  $\text{Pb}^{2+}$  ion also shows a similar behavior as that for  $\text{Cd}^{2+}$  but now appreciably less pronounced, a fact that points to a less persistent lead(II) solvation shell.

The characteristic features of the  $g(r)$  function and coordination numbers are compared with reported experimental results or QM/MM calculations in Table 3. We observe that the  $\text{Cd}^{2+}$ -oxygen distance in the first coordination shell is 0.2 Å shorter than the data reported in ref 28, whereas the first minimum and the calculated coordination number agree well with the experimental values. For  $\text{Pb}^{2+}$ , our MD calculations lead to ion-water distances and coordination numbers for the first solvation shell

**TABLE 3: Characteristic Values for  $g(r)$  and Coordination Numbers of  $\text{Cd}^{2+}$  and  $\text{Pb}^{2+}$  (the Last Column Indicates the Water Model Used in Our Calculations or Where the Reference Values Were Obtained)**

ion	$r_{M1}^a$	$r_{m1}$	$N_1$	$r_{M2}$	$r_{m2}$	$N_2$	ref
Cd-O	2.08	2.80	6.01	4.26	5.20	22.20	TIP3P
Cd-O	2.09	2.83	6.13	4.25	5.03	20.63	SPC
Cd-O	2.08	2.84	5.99	4.24	5.00	20.10	SPC/E
Cd-O	2.08	2.80	5.99	4.24	5.00	20.12	TIP4P
Cd-O	2.29	2.78	6.0	4.22	5.27	12.00	28,30
Cd-H	2.75	3.30	12.03	4.86	5.80	55.00	TIP3P
Cd-H	2.78	3.36	12.27	4.83	5.69	52.60	SPC
Cd-H	2.77	3.30	11.97	4.81	5.72	53.00	SPC/E
Cd-H	2.76	3.26	12.00	4.80	5.66	50.39	TIP4P
Cd-H	3.03			4.85		30	
Pb-O	2.58	3.50	8.45	4.83	5.95	32.00	TIP3P
Pb-O	2.60	3.51	8.53	4.80	5.89	31.21	SPC
Pb-O	2.56	3.50	8.13	4.79	5.72	28.72	SPC/E
Pb-O	2.61	3.48	8.78	4.81	5.72	29.00	TIP4P
Pb-O	2.60	3.65	9.0	5.00	6.40	24.30	29
Pb-H	3.22	3.85	17.13	5.35	6.52	77.30	TIP3P
Pb-H	3.24	3.90	17.37	5.34	6.43	74.43	SPC
Pb-H	3.26	3.90	16.73	5.32	6.38	72.50	SPC/E
Pb-H	3.25	3.91	17.87	5.30	6.35	71.96	TIP4P
Pb-H	3.25	4.00	18.00	5.35	6.40	57.60	29

<sup>a</sup>  $r_{M1}$ ,  $r_{M2}$ ,  $r_{m1}$ , and  $r_{m2}$  are the first and second maxima and first and second minima, respectively, of the  $g(r)$  function.  $N_1$  and  $N_2$  are the coordination numbers for the first and second coordination shells.

that are quite similar to corresponding values obtained from QM/MM calculations.<sup>29</sup> For both ions, the characteristic distances of the second solvation shell agree with the corresponding ones reported in the literature. The less satisfactory agreement between our results and available data for the second solvation shell coordination numbers can be ascribed to the difficulties in characterizing this much looser coordination layer. It must be kept in mind that the ion parametrization is the result of a tradeoff in the attempt to adjust two kinds of physical properties, namely, thermodynamic and structural. The very nature of the procedure prevents one from obtaining, with the same parameters, the best fit to both properties, and one chooses a compromise that simultaneously minimizes the misfit to both of them.

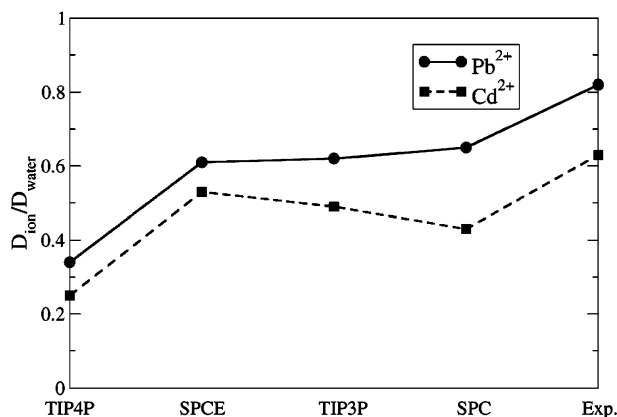
**Dynamical Properties.** In aqueous ionic solutions, the strong interaction of the solute with the water molecules results in well-defined coordination shells, as shown by the  $g(r)$  analysis, but a more detailed description of the solvation shells can be achieved by calculating dynamical properties (such as the self-diffusion coefficient and the mean residence time). The diffusion coefficient,  $D_{\text{ion}}$ , provides quantitative information, experimentally verifiable, on the Brownian motion of the ion in the solution. Again, this strongly depends on the interaction of the ion with the surrounding solvent molecules, especially the ones in the first solvation shell. The self-diffusion coefficient for the four water models considered<sup>39</sup> as well as our calculated values for  $\text{Cd}^{2+}$  and  $\text{Pb}^{2+}$  ions are included in Table 4.

Since the calculated  $\text{H}_2\text{O}$  self-diffusion coefficient varies with the water model and the ion dynamics is influenced by the solvent environment, a direct comparison of the calculated ion diffusion coefficient with experimental data is not possible. To elucidate this behavior, we plot in Figure 4 the  $D_{\text{ion}}/D_{\text{water}}$  ratios for the four water models considered (values in Table 4). For comparison, the figure also shows the corresponding experimental ratios. It can be seen that the theoretical ratios obtained from our simulations are less than the experimental values, however, the dependence on different water models is basically the same for the two ions. For the four-site TIP4P model, the  $D_{\text{ion}}/D_{\text{water}}$  ratio is smaller than the values obtained for the three-



**TABLE 4:** Calculated and Experimental Diffusion Coefficients (in 10<sup>-5</sup> cm<sup>2</sup>/s) for Pb<sup>2+</sup> ( $D_{\text{Pb}^{2+}}$ ) and Cd<sup>2+</sup> ( $D_{\text{Cd}^{2+}}$ ) Ions (the  $D_{\text{water}}$  Column Shows the Calculated and Experimental Water Self-Diffusion Coefficients)

water model	$D_{\text{Pb}^{2+}}$	$D_{\text{Cd}^{2+}}$	$D_{\text{water}}^a$	$D_{\text{Pb}^{2+}}/D_{\text{water}}$	$D_{\text{Cd}^{2+}}/D_{\text{water}}$
SCP	2.49	1.65	3.85	0.65	0.43
SCP/E	1.52	1.33	2.49	0.61	0.53
TIP3P	3.21	2.54	5.19	0.62	0.49
TIP4P	1.13	0.83	3.29	0.34	0.25
exptl <sup>b</sup>	1.890	1.438	2.30	0.82	0.625

<sup>a</sup> Reference 39. <sup>b</sup> References 40 and 41.**Figure 4.**  $D_{\text{ion}}/D_{\text{water}}$  ratios for Pb<sup>2+</sup> and Cd<sup>2+</sup> ions calculated with different water models and corresponding experimental values.

site models, namely, SPC, SPC/E, and TIP3P, hence showing that the MSD of the ions is influenced by the additional site of the TIP4P model. The self-diffusion coefficients obtained with the three-site water models lead to nearly the same proportionality with relation to  $D_{\text{water}}$ , a result that confirms the consistency of our models.

In agreement with calculations<sup>32</sup> and experimental data<sup>40</sup> reported for monovalent ions, our self-diffusion coefficient values show that despite the smaller size of Cd<sup>2+</sup> this ion exhibits a slower translational dynamics as compared with the larger-sized Pb<sup>2+</sup> ion. This can be traced to a more strongly bound and persistent first solvation shell around Cd<sup>2+</sup> as compared with Pb<sup>2+</sup>. In an attempt to rationalize this observation, we proceeded to calculate the solvent residence times around both ions.

In the calculation of  $S(t)$ , we defined the ion first hydration shell as the water molecules whose ion–O<sub>w</sub> distances are below the corresponding first minimum of  $g(r)$  (column  $r_{\text{m1}}$  in Table 3). Our calculations show that for Cd<sup>2+</sup> the first solvation shell remains stable for all water models considered and all along the 5 ns simulation, a result that suggests a much longer mean residence time. This happens because the strong Cd<sup>2+</sup>–water interaction, due to the small cadmium ionic radius, prevents significant solvent molecule exchange between the first solvation shell and the bulk. The phenomenon may therefore be rationalized by considering that what really diffuses in the solution, at least in the time scales attainable by our simulations, is not merely the bare Cd<sup>2+</sup> but this ion tightly enclosed within its first solvation shell. This behavior was already observed in other small radius divalent ions like Ca<sup>2+</sup><sup>42</sup> and leads to the smaller diffusion coefficient observed for Cd<sup>2+</sup> as compared with the one obtained for Pb<sup>2+</sup>.

During the  $S(t)$  calculations for the Pb<sup>2+</sup> ion, different values of intermittence time within the 0–10 ps time range were used. It was observed that  $S(t)$  exhibits progressively less variation as  $t^*$  increases from 0 to 2 ps, and for values longer than 2 ps,

**TABLE 5:** Mean Residence Times for the First Solvation Shell of Pb<sup>2+</sup> ( $\tau_{\text{Pb}^{2+}}$ ) for Different Water Models and Intermittence Times

water model	$\tau_{\text{Pb}^{2+}}$ (ps)		
	$t^* = 0$ ps	$t^* = 2$ ps	$t^* = 10$ ps
SPC	104	133	134
SPC/E	192	227	228
TIP3P	93	133	134
TIP4P	82	142	149

the obtained survival function became independent of  $t^*$ . This behavior leads one to assume a mean residence time of solvent molecules in the first coordination shell as the value of  $\tau_{\text{ion}}$  obtained when  $t^* = 2$  ps. This choice of the intermittence time is also justified by Impey et al.<sup>32</sup> by the fact that it is nearly equal to the residence time calculated for pure water ( $\bar{\tau}_{\text{bulk}}^S = 1.8$  ps). There it is argued that for ions that exhibit residence times considerably longer than 2 ps, as in the case of divalent ions, the residence times calculated for  $t^*$  equal to 0 or 2 ps should be close to each other, a proposition not verified in our simulations.

We show in Table 5 the mean residence times for the first solvation shell around the Pb<sup>2+</sup> ion, calculated for  $t^*$  values equal to 0, 2, and 10 ps. The obtained values turned out to be of the order of hundreds of ps, a finding consistent with the values reported for other large radius divalent ions.<sup>42</sup> The results indicate that the residence time for  $t^* = 0$  ps and  $t^* = 2$  ps presents substantial variations, hence suggesting that even for divalent ions there are important structural fluctuations in the solvation shells. As already mentioned, the residence times calculated for  $t^* = 2$  ps and  $t^* = 10$  ps do not exhibit significant variations.

## Conclusions

We present new Lennard-Jones parameters for Cd<sup>2+</sup> and Pb<sup>2+</sup> ion–water interactions. They are determined by adjusting them to simultaneously reproduce thermodynamic and structural properties from experimental or QM/MM results. The transferability of these parameters is confirmed by performing additional simulations employing different water models. Dynamical properties were calculated and compared with available experimental data to validate our parametrization. The proposed methodology uses the LIE method to calculate absolute hydration free energies rather than the thermodynamic ones usually applied in related works. Our results, obtained at a much less computational cost, are nevertheless in good agreement with experimental data. The main feature of our methodology is to focus on both thermodynamic and structural properties to adjust the final parameters, a procedure that renders confidence to the obtained results. On the other hand, this approach may in some cases lead to intrinsic errors which, however, are small enough not to invalidate the results of the present work.

With regards to structural properties, the proposed parameters are shown to be transferable among the SPC, SPC/E, TIP3P, and TIP4P water models. The transferability also holds when computing absolute free energy with three-site interacting water models. A rather less satisfactory result is found when employing the four-site TIP4P water model. The ion self-diffusion coefficients were computed and compared with experimental data to cross-validate the determined parameters. The MD results that better compare with experimental data are those obtained from the SPC/E water model. This model, in turn, exhibits a self-diffusion coefficient that closely approaches the experimental value found for water. The  $D_{\text{ion}}/D_{\text{water}}$  ratios were almost

the same for the three-site water models, a fact that provides further support to the parameters consistency. The survival probability function,  $S(t)$ , and our estimate of the mean residence time of solvent molecules in the ion solvation shell show a striking different behavior for the two ions modeled in this work. For  $\text{Pb}^{2+}$ , we found a relative persistence solvation shell with a mean residence time of hundreds of ps. In contrast, the stronger water– $\text{Cd}^{2+}$  interaction prevents the solvent molecules from leaving the first solvation shell, at least during the time scales probed by our simulations, leading to a larger effective hydration radius and therefore a smaller diffusion coefficient.

**Acknowledgment.** The authors thank Ernesto Raul Cafarena for the valuable discussion and critical reading of the manuscript. A.S.d.A. and M.T.S. acknowledge the financial support provided by the Brazilian agency FAPESP (projects 01/10750-0 and 05/53931-5, respectively). The authors thank the European Commission for the financial support provided under contract IAC3–CT–2000–30006.

## References and Notes

- (1) Barrie, L. A.; Gregor, D.; Hargrave, B.; Lake, R.; Muir, D.; Shearer, R.; Tracey, B.; Bidleman, T. *Sci. Total Environ.* **1992**, *122*, 1.
- (2) MacDonald, R. W.; Barrie, L. A.; Bidleman, T. F.; Diamond, M. L.; Gregor, D. J.; Semkin, R. G.; Strachan, W. M. J.; Li, Y. F.; Wania, F.; Alae, M.; Alexeeva, L. B.; Backus, S. M.; Bailey, R.; Bewers, J. M.; Gobeil, C.; Halsall, C. J.; Harner, T.; Hoff, J. T.; Jantunen, L. M. M.; Lockhart, W. L.; Mackay, D.; Muir, D. C. G.; Pudykiewicz, J.; Reimer, K. J.; Smith, J. N.; Stern, G. A.; Schroeder, W. H.; Wagemann, R.; Yunker, M. B. *Sci. Total Environ.* **2000**, *254*, 93.
- (3) Muir, D. C. G.; Wagemann, R.; Hargrave, B. T.; Thomas, D. J.; Peakall, D. B.; Norstrom, R. J. *Sci. Total Environ.* **1992**, *122*, 75.
- (4) Rhue, R. D.; Mansell, R. S.; Ou, L. T.; Cox, R.; Tang, S. R.; Ouyang, Y. *Crit. Rev. Environ. Control* **1992**, *22*, 169.
- (5) Hare, L. *Crit. Rev. Toxicol.* **1992**, *22*, 327.
- (6) Singh, R. P.; Tripathi, R. D.; Sinha, S. K.; Maheshwari, R.; Srivastava, H. S. *Chemosphere* **1997**, *34*, 2467.
- (7) Chiba, M.; Masironi, R. *Bull. WHO* **1992**, *70*, 269.
- (8) Dudka, S.; Miller, W. P. *J. Environ. Sci. Health, Part B* **1999**, *34*, 681.
- (9) McLaughlin, M. J.; Tiller, K. G.; Naidu, R.; Stevens, D. P. *Aust. J. Soil Res.* **1996**, *34*, 1.
- (10) Spry, D. J.; Wiener, J. G. *Environ. Pollut.* **1991**, *71*, 243.
- (11) Porter, S. K.; Scheckel, K. G.; Impellitteri, C. A.; Ryan, J. A. *Crit. Rev. Environ. Sci. Technol.* **2004**, *34*, 495.
- (12) Aqvist, J. *J. Phys. Chem.* **1990**, *94*, 8021.
- (13) Chandrasekhar, J.; Spellmeyer, D. C.; Jorgensen, W. L. *J. Am. Chem. Soc.* **1984**, *106*, 903.
- (14) Reichert, D. E.; Norrby, P. O.; Welch, M. J. *Inorg. Chem.* **2001**, *40*, 5223.
- (15) van Veggel, F. C. J. M.; Reinhoudt, D. N. *Chem.—Eur. J.* **1999**, *5*, 90.
- (16) Allinger, N. L.; Zhou, X. F.; Bergsma, J. *THEOCHEM* **1994**, *118*, 69.
- (17) Rappe, A. K.; Casewit, C. J.; Colwell, K. S.; Goddard, W. A.; Skiff, W. M. *J. Am. Chem. Soc.* **1992**, *114*, 10024.
- (18) Babu, C. S.; Lim, C. J. *Phys. Chem. A* **2006**, *110*, 691.
- (19) Jorgensen, W. L.; Maxwell, D. S.; TiradoRives, J. *J. Am. Chem. Soc.* **1996**, *118*, 11225.
- (20) Oostenbrink, C.; Villa, A.; Mark, A. E.; Van, Gunsteren, W. F. *J. Comput. Chem.* **2004**, *25*, 1656.
- (21) Weiner, S. J.; Kollman, P. A.; Case, D. A.; Singh, U. C.; Ghio, C.; Alagona, G.; Profeta, S.; Weiner, P. *J. Am. Chem. Soc.* **1984**, *106*, 765.
- (22) Jorgensen, W. L.; Chandrasekhar, J.; Madura, J. D.; Impey, R. W.; Klein, M. L. *J. Chem. Phys.* **1983**, *79*, 926.
- (23) Berendsen, H. J. C.; Postma, J. M. P.; van Gunsteren, W. F.; Hermans, J. In *Jerusalem Symposia on Quantum Chemistry and Biochemistry*; Pullman, B., Ed.; Reidel: Dordrecht, Holland, 1981.
- (24) Berendsen, H. J. C.; Grigera, J. R.; Straatsma, T. P. *J. Phys. Chem.* **1987**, *91*, 6269.
- (25) Aqvist, J.; Medina, C.; Samuelsson, J. E. *Protein Eng.* **1994**, *7*, 385.
- (26) Torrie, G. M.; Valleau, J. P. *Chem. Phys. Lett.* **1974**, *28*, 578.
- (27) Burgess, J. *Metal ions in solution*; Ellis Horwood, distributed by Halsted Press: Chichester, U.K., New York, 1978.
- (28) Bol, W.; Gerrits, G. J. A.; Panthale, C. *J. Appl. Crystallogr.* **1970**, *3*, 486.
- (29) Hofer, T. S.; Rode, B. M. *J. Chem. Phys.* **2004**, *121*, 6406.
- (30) Kritayakornpong, C.; Plankensteiner, K.; Rode, B. M. *J. Phys. Chem. A* **2003**, *107*, 10330.
- (31) Allen, M. P.; Tildesley, D. J. *Computer simulation of liquids*; Clarendon Press, Oxford University Press: Oxford, U.K., New York, 1987.
- (32) Impey, R. W.; Madden, P. A.; McDonald, I. R. *J. Phys. Chem.* **1983**, *87*, 5071.
- (33) Kirkwood, J. G. *J. Chem. Phys.* **1935**, *3*, 300.
- (34) Leach, A. R. *Molecular modelling: principles and applications*, 2nd ed.; Prentice Hall: Harlow, U.K., New York, 2001.
- (35) Aqvist, J.; Luzhkov, V. B.; Brandsdal, B. O. *Acc. Chem. Res.* **2002**, *35*, 358.
- (36) Hansson, T.; Marelus, J.; Aqvist, J. *J. Comput.-Aided Mol. Des.* **1998**, *12*, 27.
- (37) Floris, F. M.; Selmi, M.; Tani, A.; Tomasi, J. *J. Chem. Phys.* **1997**, *107*, 6353.
- (38) Van, der Spoel, D.; Lindahl, E.; Hess, B.; Groenhof, G.; Mark, A. E.; Berendsen, H. J. C. *J. Comput. Chem.* **2005**, *26*, 1701.
- (39) Mahoney, M. W.; Jorgensen, W. L. *J. Chem. Phys.* **2001**, *114*, 363.
- (40) Lide, D. R., Ed. *CRC Handbook of Chemistry and Physics*, 84th ed.; CRC Press: Boca Raton, FL, 2003.
- (41) Eisenberg, D. S.; Kauzmann, W. *The structure and properties of water*; Clarendon Press: Oxford, U.K., 1969.
- (42) Obst, S.; Bradaczek, H. *J. Phys. Chem.* **1996**, *100*, 15677.